Identification of a Novel Pyrazolo[3,4-*d*]pyrimidine Able To Inhibit Cell Proliferation of a Human Osteogenic Sarcoma in Vitro and in a Xenograft Model in Mice†

Fabrizio Manetti,[‡,¶] Annalisa Santucci,[§,¶] Giada A. Locatelli,[#] Giovanni Maga,[#] Adriano Spreafico,[⊥] Tommaso Serchi,[§] Maurizio Orlandini,[§] Giulia Bernardini,[§] Nicola P. Caradonna,[||] Andrea Spallarossa,[⊗] Chiara Brullo,[⊗] Silvia Schenone,*[,⊗] Olga Bruno,[⊗] Angelo Ranise,[⊗] Francesco Bondavalli,[⊗] Oskar Hoffmann,[△] Mauro Bologna,[▽] Adriano Angelucci,[▽] and Maurizio Botta[‡]

Dipartimento Farmaco Chimico Tecnologico, Università degli Studi di Siena, via Alcide de Gasperi 2, I-53100 Siena, Italy; Dipartimento di Biologia Molecolare, Università degli Studi di Siena, via Fiorentina 1, I-53100 Siena, Italy; Istituto di Genetica Molecolare, IGM-CNR, via Abbiategrasso 207, I-27100 Pavia, Italy; Dipartimento di Medicina Clinica e Scienze Immunologiche, Policlinico Le Scotte, Università degli Studi di Siena, I-53100 Siena, Italy; Siena Biotech, Via Fiorentina 1, I-53100 Siena, Italy; Dipartimento di Scienze Farmaceutiche, Università degli Studi di Genova, viale Benedetto XV 3, I-16132 Genova, Italy; Department of Pharmacology and Toxicology, University of Vienna, Althanstrasse 14, A-1090 Vienna, Austria; and Dipartimento di Biologia di Base ed Applicata, Università degli Studi dell'Aquila, Via Vetoio, Loc. Coppito, I-67010 Coppito L'Aquila, Italy

Received December 20, 2006

New pyrazolo[3,4-*d*]pyrimidines were synthesized and found to inhibit Src phosphorylation in a cell-free assay. Some of them significantly reduced the growth of human osteogenic sarcoma (SaOS-2) cells. The best compound, in terms of inhibitory properties toward both Src and SaOS-2 cells, was further investigated and found to reduce bone resorption when used to treat mouse osteoclasts, without interfering with normal osteoblast growth. Moreover, its metabolic stability prompted its study on a human SaOS-2 xenograft tumor model in nude mice, where the compound reduced significantly both the volume and weight of the tumor. These experimental findings make the new compound an interesting hit in the field of bone-related diseases.

Introduction

Osteoblasts and osteoclasts are involved in the dynamic and highly regulated processes of bone remodeling, through a variety of cellular signaling pathways involving protein kinases. Among the latter, the tyrosine kinase Src has been demonstrated to play a crucial regulatory role in both osteoblasts and osteoclasts. In particular, Src has been implicated as a negative regulator of osteoblast functional activity, on the basis of the fact that reduction of Src expression stimulates osteoblast differentiation and bone formation.[1] Conversely, Src is also a mediator of anti-apoptotic signaling in osteoblasts, induced by various factors. As examples, Wnt proteins prevent apoptosis, prolonging the survival of osteoblasts through the activation of the Src signaling cascade.[2] Moreover, anti-apoptotic effects of vitamin D3 analogues on the same cells are blocked by Src inhibitors such as 4-amino-5-(4-methylphenyl)-7-(*tert*-butyl)pyrazolo[3,4-*d*]pyrimidine (PP1).[3] On the other hand, disruption of the *src* gene leads to osteopetrosis in mice,[4] due to the inability of osteoclasts to form ruffled borders and resorb bone during one of the final stages of their maturation (positive regulatory role of Src).[5] In addition, Src is also involved in signaling pathways leading to cell death of malignant osteoblasts (such as the osteosarcoma SaOS-2 cell line)[6] and contributes, in combination with paxillin, to the high metastatic potential of the human osteosarcoma HuO9 cell line.[7] All of these experimental data make Src an attractive and promising therapeutic target for the treatment of bone-related diseases such as osteoporosis,[8−10] osteosarcoma,[11] and cancer-induced bone metastasis.[7]

Recent literature reports a plethora of Src inhibitors originated from a variety of molecular scaffolds that have demonstrated potency up to the nanomolar range in enzymatic assays and high efficacy in animal models of bone disease. Such compounds are classified into SH2−SH3 domain inhibitors and kinase domain inhibitors. The first ones block protein−protein interactions between Src and other proteins involved in the signaling pathways. As an example, blocking the SH2 domain with high affinity might attenuate the excessive signal transduction in bone resorption diseases, such as osteoporosis and related bone diseases.[12] On the other hand, many of the Src kinase domain inhibitors belong to 6−6 and 5−6 bicyclic cores, such as quinolines,[13] quinazolines,[14] pyrrolo[2,3-*d*]pyrimidine,[15] and pyrazolo[3,4-*d*]pyrimidine.[16] In this context, we have recently described several pyrazolo[3,4-*d*]pyrimidines endowed with in vitro antiproliferative and pro-apoptotic activity toward epidermoid (A431) and breast cancer (8701-BC) cell lines, acting through the inhibition of c-Src phosphorylation.[17] In particular, compound **1** (Table 1) showed a submicromolar activity toward isolated Src and an inhibitory activity about 2-fold better than that of the reference compound 4-amino-5-(4-chlorophenyl)-7-(*tert*-butyl)pyrazolo[3,4-*d*]pyrimidine (PP2) against both A431 and 8701-BC cells.[17] Continuing our efforts in the field of Src inhibitors, **1** was chosen as the parent compound to design and synthesize new pyrazolo[3,4-*d*]-pyrimidines (**2**−**25**) that, on the basis of our previous findings, were expected to interfere with Src activity. Accordingly, they were evaluated in a cell-free Src assay. Moreover, due to the

* Author to whom correspondence should be addressed (telephone 0039 010 3538866; fax 0039 010 3538358; e-mail schensil@unige.it).

† Dedicated to Professor Fulvio Gualtieri on the occasion of his 70th birthday.

‡ Dipartimento Farmaco Chimico Tecnologico, Università degli Studi di Siena.

§ Dipartimento di Biologia Molecolare, Università degli Studi di Siena.

¶ These authors contributed equally to this work.

Istituto di Genetica Molecolare, IGM-CNR.

⊥ Dipartimento di Medicina Clinica e Scienze Immunologiche, Policlinico Le Scotte, Università degli Studi di Siena.

|| Siena Biotech.

⊗ Dipartimento di Scienze Farmaceutiche, Università degli Studi di Genova.

△ Department of Pharmacology and Toxicology, University of Vienna.

▽ Dipartimento di Biologia di Base ed Applicata, Università degli Studi dell'Aquila.

10.1021/jm061449r CCC: $37.00
Published on Web 10/11/2007

Table 1. Structure, Physicochemical Properties, and Biological Data of Test Compounds

compd	R	R^1	R^2	mp	yield	K_i[a]	CV (%)[b] after 24 and 48 h
1[c,d]	MeS	$C_6H_5(CH_2)_2$	H	73−74	76	0.7 ± 0.1	102.7 ± 1.9; 99.5 ± 0.9
2	MeS	*m*-F−$C_6H_4(CH_2)_2$	H	111−112	73	13 ± 3	101.1 ± 1.1; 100.8 ± 2.1
3	MeS	*o*-Cl−$C_6H_4(CH_2)_2$	H	99−100	70	4.0 ± 1.7	102.9 ± 1.3; 100.5 ± 0.5
4	MeS	*m*-Cl−$C_6H_4(CH_2)_2$	H	122−123	68	6.0 ± 2.1	80.6 ± 0.7; 39.3 ± 2.0
5	MeS	*p*-Cl−$C_6H_4(CH_2)_2$	H	99−100	70	25 ± 4	85.2 ± 0.7; 75.4 ± 1.3
6	MeS	*p*-Me−$C_6H_4(CH_2)_2$	H	99−100	71	15 ± 2	101.9 ± 1.9; 96.3 ± 1.1
7	MeS	*p*-MeO−$C_6H_4(CH_2)_2$	H	60−61	62	4.0 ± 1.3	101.0 ± 3.0; 49.8 ± 2.1
8	MeS	$C_6H_5(CH_2)_2$	Cl	127−129	71	2.8 ± 1.2	99.9 ± 0.9; 89.4 ± 2.3
9	EtS	$C_6H_5(CH_2)_2$	H	99−100	82	7.5 ± 2.7	107.3 ± 3.5; 22.2 ± 1.3
10[c]	MeS	$C_6H_5CH_2$	H	142−143	81	3.7 ± 0.9	92.8 ± 1.3; 26.8 ± 1.2
11	MeS	*o*-Cl−$C_6H_4CH_2$	H	158−159	80	3.1 ± 1.4	101.7 ± 0.9; 102.1 ± 1.2
12	MeS	*p*-Cl−$C_6H_4CH_2$	H	126−127	75	24 ± 5	113.4 ± 1.5; 54.9 ± 2.4
13	MeS	*o*-F−$C_6H_4CH_2$	H	133−134	72	21 ± 4	104.1 ± 1.3; 99.7 ± 0.4
14	MeS	*m*-F−$C_6H_4CH_2$	H	113−114	71	5.2 ±1.1	106.2 ± 3.0; 71.3 ± 2.1
15	MeS	*p*-F−$C_6H_4CH_2$	H	136−137	68	4.6 ± 1.7	102.1 ± 1.4; 99.2 ± 1.0
16	MeS	$C_6H_5CH_2$	Cl	130−131	74	3.0 ± 1.0	52.2 ± 2.4; 24.4 ± 2.5
17	MeS	$C_6H_5CH_2$	F	152−153	74	35 ± 8	62.7 ± 0.7; 44.4 ± 2.5
18[d]	MeS	*m*-Cl−C_6H_4	H	102−103	55	0.6 ± 0.1	17.1 ± 1.3; 15.1 ± 0.7
19	MeS	*m*-F−C_6H_4	H	212−213	43	1.4 ± 0.3	94.8 ± 2.7; 84.3 ± 1.5
20	MeS	*m*-Br−C_6H_4	H	250 (dec)	40	1.8 ± 0.2	100.1 ± 1.1; 84.7 ± 0.3
21	MeS	C_6H_5	H	169−170	60	1.2 ± 0.3	100.1 ± 1.2; 94.4 ± 0.7
22[d]	EtS	*m*-Cl−C_6H_4	H	216−217	55	0.5 ± 0.1	76.5 ± 1.9; 44.3 ± 1.8
23	PrS	*m*-Cl−C_6H_4	H	214−215	52	1.2 ± 0.4	77.8 ± 3.0; 68.4 ± 1.9
24	H	*m*-Cl−C_6H_4	H	202−203	62	3.8 ± 1.7	104.1 ± 0.4; 101.3 ± 1.5
25	MeS	*m*-Br−C_6H_4	F	224−225	45	4.1 ± 0.8	63.1 ± 1.1; 55.4 ± 2.0
PP2						0.5 ± 0.1	36.8 ± 1.7; 36.4 ± 1.6

[a] K_i (expressed as a μM concentration) toward recombinant human Src was calculated according to the following equation: $K_i = (ID_{50} - E_0/2)/\{E_0 - [S_0/K_m - 1]/E_0\}$, where S_0 is the concentration of the competing substrate (ATP) and E_0 is the concentration of the enzyme. Each experiment was in triplicate, and mean values were used for the interpolation. Curve fitting was performed with the program GraphPad Prism. [b] Antiproliferative activity of test compounds (12.5 μM) toward SaOS-2 cells (MTT assay) after 24 and 48 h of treatment, expressed as cellular viability (CV, %) with respect to control (100%). Values are means ± SD of three independent experiments performed in duplicates. [c] Compounds reported elsewhere.[17] [d] Although **18** and **22** have comparable K_i values for Src inhibition, they show significantly different activities in the cell proliferation assay. Because the replacement of the MeS group with an EtS moiety is expected to have not a great effect on either the solubility (calculated solubilities are −6.53 and −6.82, respectively; Table 2) or the metabolic stability, a reason of the discrepancy in K_i values and cell proliferation activity may be that **22** is able to inhibit Akt less (by 68%) than what **18** does (quantitative inhibition). However, the biological behavior of **22** deserves further investigations. Similarly, the biological properties of **1** are not completely understood, yet. In fact, such a compound, with a 0.7 μM K_i toward Src, was previously demonstrated to have inhibitory properties toward several cell lines presumably via Src-dependent mechanisms (see ref 17), whereas it is completely unable to inhibit SaOS-2 proliferation.

role of Src in osteoblast and osteoclast growth, some compounds were also tested for their inhibitory properties toward human osteoblasts (both normal and osteosarcoma SaOS-2 cell lines) and osteoclasts. As a result, one compound (**18**) emerged for its marked ability to reduce the viability of SaOS-2 cells in vitro, without affecting normal osteoblasts. It also showed metabolic stability in a Tier 1 metabolic stability screen. These experimental findings prompted us to test it on a human SaOS-2 xenograft tumor in nude mice, resulting in a significant reduction of both the volume and weight of the tumor.

Chemistry

Compounds **1**−**23** and **25** were prepared as reported in Scheme 1, according to procedures previously described.[17] The starting products were the 2-hydrazinoethanols **26a**−**c**, obtained by starting from the appropriate phenyloxirane, following a reported procedure.[18] Reaction of **26a**−**c** with ethyl(ethoxymethylene)cyanoacetate afforded the ethyl esters of 5-amino-1*H*-pyrazole-4-carboxylic acids **27a**−**c**, which were in turn treated with benzoyl isothiocyanate in THF at reflux for 12 h to give **28a**−**c**. These intermediates were cyclized to the pyrazolo[3,4-*d*]pyrimidinones **29a**−**c** by treatment with 2 M NaOH at 100 °C for 10 min, followed by acidification with acetic acid. Alkylation of the thio group at position 6 with the appropriate alkyl iodide in THF at reflux afforded the 6-alkylthio derivatives **30a**−**e**, which were in turn treated with the Vilsmeier complex ($POCl_3$:DMF, 4 equiv) in $CHCl_3$ to obtain the dihalogenated compounds **31a**−**e**, bearing a chlorine atom both at position 4 of the pyrimidine nucleus and at the N1 side chain. These compounds were purified in good yield by chromatography on a Florisil column. Finally, reaction of **31a**−**c** with an excess of various amines in toluene at rt afforded compounds **1**−**17** in yields ranging from 60 to 80%. The aniline derivatives **18**−**23** and **25** were obtained by reaction between **31a**−**e** and the appropriate amine in ethanol at reflux for 3 h.

The 6-unsubstituted derivative **24** was obtained by reaction of **32**, synthesized following our reported procedure,[19] and *m*-chloroaniline in ethanol at reflux for 3 h (Scheme 2).

Biology

Inhibition of SaOS-2 Proliferation. The new compounds were evaluated for their ability to inhibit proliferation of the human osteosarcoma SaOS-2 cell line through a preliminary MTT assay (25 μM test dose, 24 and 48 h treatments), using PP2 as the reference compound (Table 1).[20] As a result, although several compounds (namely, **16**, **17**, **18**, and **25**) were able to reduce cell viability upon a 24 h treatment, the sole compound **18** dramatically reduced cell proliferation to about 17% after 24 h and to about 15% after 48 h, with respect to control. In comparison, percent of cell growth allowed by PP2 is about 37 and 36% after 24 and 48 h, respectively. Moreover, IC_{50} values were determined on the basis of seven test concentrations in the range between 1 and 100 μM. Results showed a dose-dependent inhibitory activity, with IC_{50} values of 8.1 and 12.6 μM for PP2 and **18**, respectively.

Inhibition of Src Activity in a Cell-Free Assay. Because pyrazolo[3,4-*d*]pyrimidines were previously found to inhibit Src activity,[17] we tested the new compounds on a cell-free assay to assess their ability to influence the enzymatic activity of Src. Biological data reported in Table 1 showed that compounds were

Scheme 1

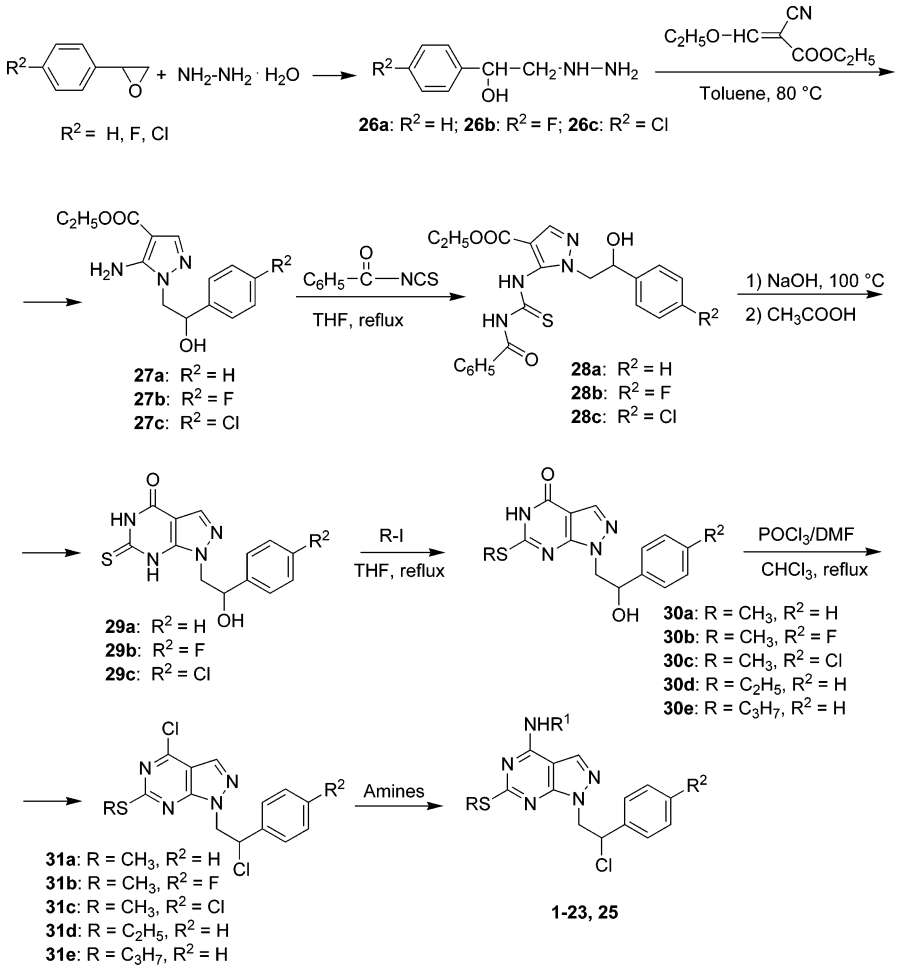

Scheme 2

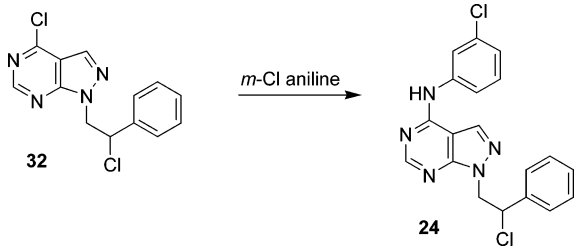

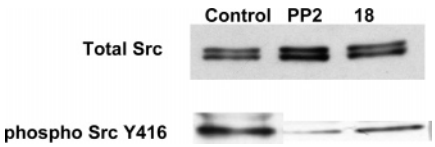

Figure 1. PP2 and **18** abolish Src-Tyr416 phosphorylation. Compounds were used at their corresponding IC_{50}. Cells were treated for 2 h prior to their lysis. Specific Src phosphorylation was evaluated when whole-cell lysates were immunoprobed with anti-total Src, anti-non-phospho-Src-Y416, and anti-phospho-Src-Y416 antibodies. Results are representative of three independent experiments.

competitive with the ATP substrate but not with a peptide used as an Src substrate.[21] In detail, the introduction of a substituent on the phenyl ring of the C4 side chain (compounds **2**−**7**) led to a significant drop in affinity with respect to the parent compound **1**. In a similar way, transforming the N1 side chain (**8**) and increasing the bulkiness of the substituent at C6 from a methylthio to an ethylthio group (**9**) were detrimental for affinity, despite these compounds retaining a micromolar K_i value. Shortening the C4 phenylethylamino side chain to a benzylamino group (**10**) and introducing substituents at the benzyl moiety (**11**−**15**) led to a lower affinity. Activity in the micromolar range was also found for derivatives of **10**, in which an additional halogen was introduced at the N1 side chain (**16** and **17**). On the contrary, the anilino derivative **18** was characterized by one of the best affinity values toward Src (0.6 μM), comparable to that of the parent compound **1**. On this basis, to evaluate the influence of the molecular portions of **18** in Src inhibition, several derivatives were synthesized and tested. When the chlorine group at the anilino moiety was changed into F, Br, and H (**19**, **20**, and **21**, respectively), activity underwent only a slight decrease (1.4, 1.8, and 1.2 μM, respectively). Similarly, **22** and **23**, bearing a bulkier substituent at position 6, showed activities of 0.5 and 1.2 μM (comparable to that of **18**), respectively, whereas the C6-unsubstituted derivative **24** had a 4-fold lower activity (3.8 μM). Insertion of an additional halogen substituent on the N1 side chain led to **25** with a 2-fold decrease in affinity, in comparison to **20**.

Inhibition of Src Phosphorylation. To determine whether the new compounds were able to inhibit the phosphorylation of Src at the level of Tyr416, we used specific anti-Src antibodies toward total Src and toward Src with phosphorylated Tyr416. Treatment with both PP2 and **18** (chosen as the hit compound, on the basis of its highest activity in both enzymatic and cellular assays) led to a marked reduction (77 and 62%, respectively) of Tyr416 phosphorylation (Figure 1), suggesting that inhibition of SaOS-2 cell proliferation was modulated, at least in part, by Src.

Table 2. Log *P*, Solubility, and Membrane Permeability of Test Compounds

compd	log *P*[a]	solubility[b]	Caco2[c]
1	5.55 (5.46)	−6.78	1.00
2	5.76	−6.23	0.77
3	6.22	−6.79	1.17
4	6.22	−6.74	1.08
5	6.22	−6.82	1.11
6	6.04	−6.62	1.03
7	5.54	−6.48	0.81
8	6.22	−6.66	1.01
9	5.90	−6.47	1.07
10	5.23	−6.29	0.98
11	5.90	−6.52	0.95
12	5.90	−6.88	1.00
13	5.44	−6.14	0.81
14	5.44	−6.15	0.79
15	5.44	−6.10	0.80
16	5.90	−6.45	0.96
17	5.44	−5.77	0.78
18	6.05 (6.01)	−6.53	0.97
19	5.60	−5.94	0.83
20	6.14 (6.13)	−6.85	1.03
21	5.39	−6.28	1.03
22	6.40 (6.41)	−6.82	1.07
23	6.93	−6.97	1.07
24	4.99	−5.76	0.88
25	6.34	−6.65	0.89

[a] Calculated by means of the AlogP98 method.[30] In parentheses are experimental values. [b] Solubility refers to the thermodynamic solubility model (as implemented in Volsurf).[22] Values are expressed as log[solubility], in mol/L. The overall range is $-8 < \log[\text{solubility}] < +2$, where lower values indicate poor solubility and higher values indicate highly soluble compounds. [c] Caco2 refers to the Caco2 permeation model (as implemented in Volsurf).[22] Values represent a score ranging from −1 to +1, corresponding to the following permeability values: −1 corresponds to a permeability of $<4 \times 10^{-6}$ cm/s, 0 corresponds to a permeability between 4×10^{-6} and 8×10^{-6} cm/s, and 1 corresponds to a permeability of $>8 \times 10^{-6}$ cm/s.

Metabolic Stability and Alternative Targets of 18. It is worth noting that biological data revealed several inconsistencies between cellular and enzymatic assays. In fact, essentially all of the compounds were active in the enzymatic assay within a relatively narrow range (from low to sub-micromolar concentrations). On the other hand, their activity against osteosarcoma cells varied widely, and MTT experiments demonstrated that a 25 μM concentration of the test compound was in many cases unable to interfere with the growth of SaOS-2 cells (remaining cellular viability values at 100%). Disagreement between enzymatic and cellular data allowed us to formulate several hypotheses about how compounds inhibit SaOS-2 cell growth. In particular, although compounds were able to interact directly with Src and reduce its enzymatic activity, it appeared that physicochemical properties (such as solubility, membrane permeability, log *P*) that, in turn, influence pharmacokinetic parameters in part did not allow compounds to reach Src itself within cells. A possible explanation could be a low solubility of the pyrazolo-pyrimidine derivatives in the assay conditions, which in part prevented compounds from entering cells. To check this hypothesis, the solubility profiles of such compounds were calculated by means of the software Volsurf,[22] resulting in a general low solubility (Table 2), whereas application of a Caco2 permeation model showed that compounds are well absorbed through cell membranes. Moreover, upon penetration into the cells, several events may occurr (such as an increase in drug efflux by activating the expression of the MDR1 gene, which encodes for the P-glycoprotein)[23] that lead to a partial or marked inactivation of the compounds. Alternatively, the lack of activity of some compounds toward SaOS-2 cells may also depend on their metabolic instability. An example supporting this hypothesis is represented by compound **1**, which showed an activity toward the isolated Src similar to that of **18** (0.7 vs 0.6 μM, respectively), whereas its activity on the cell-based assay was not significant. The metabolic stability of **1** was assessed by a Tier 1 profiling screen by incubation of 1 μM compound with recombinant human cytochrome P450 3A4 with and without the cofactor NADPH for 1 h at 37 °C. Following protein precipitation and filtration, the amount of remaining compound was determined by UPLC-MS and found to be 10%, allowing us to classify **1** as a metabolically instable compound.

Moreover, contradictions in biological data could also depend on the fact that cellular tests reflect the interference of a compound in steps not shown in assays aimed at evaluating the inhibition of Src activity. In other words, the enzymatic assay reports only the effect of compounds in inhibiting Src activity, whereas biological data referring to the antiproliferative activity could also depend on other events, in addition to Src inhibition. In this context, the micromolar inhibition of Src activity mediated by all of the new compounds opposed to the wide variability of cellular data also suggested that Src could not be the sole or the major target of the pyrazolo-pyrimidines. To check this hypothesis and to shed light on the mechanism of action of **18** at the molecular level, we preliminarily tested it toward a panel of 17 tyrosine kinases.[24] As a result, a 10 μM concentration of **18** was able to completely and selectively inhibit the enzymatic activity of Akt, which is known to be involved in a Src-dependent pathway found in human osteosarcoma SaOS-2 cells.[25] Moreover, activity of HER-1 and Ret was also reduced by 42%, whereas a decrease of <30% was found for the remaining kinases. On the other hand, three additional compounds (namely, **1**, **20**, and **22**), inactive in the cell-based assay, were also tested for their activity toward the kinase panel. As a result, **1** reduced activity of B-Raf-V599E by 30%, whereas percent inhibition was lower or null for the other kinases. The activity of B-Raf-V599E was slightly reduced (by 15%) also by **22**, which also partially inhibited Akt (by 68%). No significant inhibition toward the remaining kinases was found. Finally, **20** showed a 17% reduction of the HER-1 activity, without influencing the remaining kinases.

This result supported the hypothesis that inhibition of SaOS-2 growth upon treatment with **18** may result from a combination of targeting either Src or Akt.

To check if the best compound (**18**) was worthy of further in vitro and in vivo biological investigations, its metabolic stability was assessed. Upon submission of **18** to a Tier 1 screen (see above), the remaining amount of the compound was 33% of the original amount used in this assay, leading to the classification of **18** as metabolically stable.

Cytotoxicity. Because cytotoxicity may occur as an undesirable side effect of compounds with a potential therapeutic application, we evaluated viability with the Trypan blue assay. As reported in Figure 2, PP2 was found to be more cytotoxic than **18**, causing 42% reduced viability. On the contrary, **18** exerted only a minor cytotoxic effect on SaOS-2 (13% reduced viability), as also evidenced by a TUNEL assay assessing a pro-apoptotic effect of **18** (Figure 3).

Inhibition of Normal Osteoblasts. Because **18** showed an interesting inhibitory activity toward osteosarcoma cells, and with the aim of checking if such a compound deserves to be further studied as a possible lead against osteosarcoma cell lines, we planned to test it toward human normal osteoblasts. Cells were treated with the test compound (25 μM) for 48 h, following a MTT assay. Osteoblast growth was moderately reduced by **18** (20%), different from PP2, which showed a 50% inhibitory

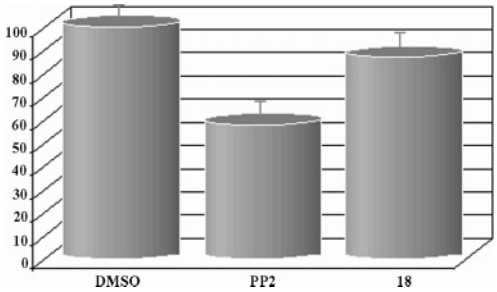

Figure 2. Cytotoxicity of PP2 and **18** toward SaOS-2 cells evaluated by the Trypan blue assay. Cells were treated with compounds at their corresponding IC_{50} for 24 h. Data are expressed as percentage of live cells with respect to control (vehicle). Values are means ± SEM of three independent experiments performed in duplicates. Error bars indicate SDs from the mean values.

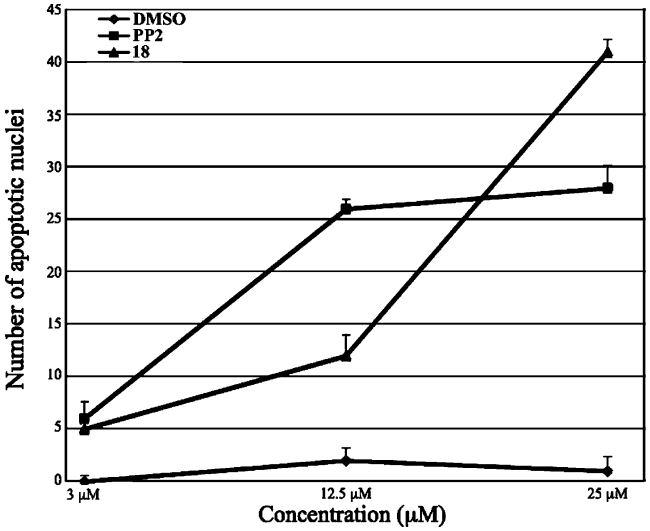

Figure 3. TUNEL assay of SaOS-2 cells after treatment with PP2 and **18** at 3, 12.5, and 25 μM for 48 h. Experiments were performed in triplicate. Standard deviations are shown as bars.

activity. It is very important to note that, at the same concentration, the new pyrazolo-pyrimidine showed an antiproliferative activity toward SaOS-2 cells of about 85%, suggesting that it is highly selective in interfering with the proliferation of abnormal osteoblasts. A time course experiment was also performed to evaluate the pro-apoptotic activity of **18**, further supporting the hypothesis that the test compound is able to specifically inhibit cell proliferation and to induce apoptosis in transformed cells with respect to normal osteoblasts.[26]

Inhibition of Osteoclasts. Considering that Src-defective osteoclasts showed abnormal organization of cytoskeletal elements necessary for bone resorption, **18** was also tested for its ability to influence osteoclast-resorptive activity, in comparison to PP2 (Figure 4). Compound **18** was able to abrogate bone resorption in mouse osteoclasts at 10 and 1 μM concentrations, whereas percent inhibition was lower but significant also for reduced test dose (up to 1 nM).

It is very important to note that there is a significant difference in bone resorption for the control (DMSO) in the two experiments reported in Figure 4. In fact, when compound **18** was tested, bone resorption in the control group was about 20%, whereas only a 3% resorption was found in the control group when PP2 was assayed. The method used to measure bone resorption is based on the growth in vitro of osteoclasts that then resorb bone. However, this cell-based assay is usually characterized by a significant variability, mainly due to the fact that the basic amount of bone resorption can vary among

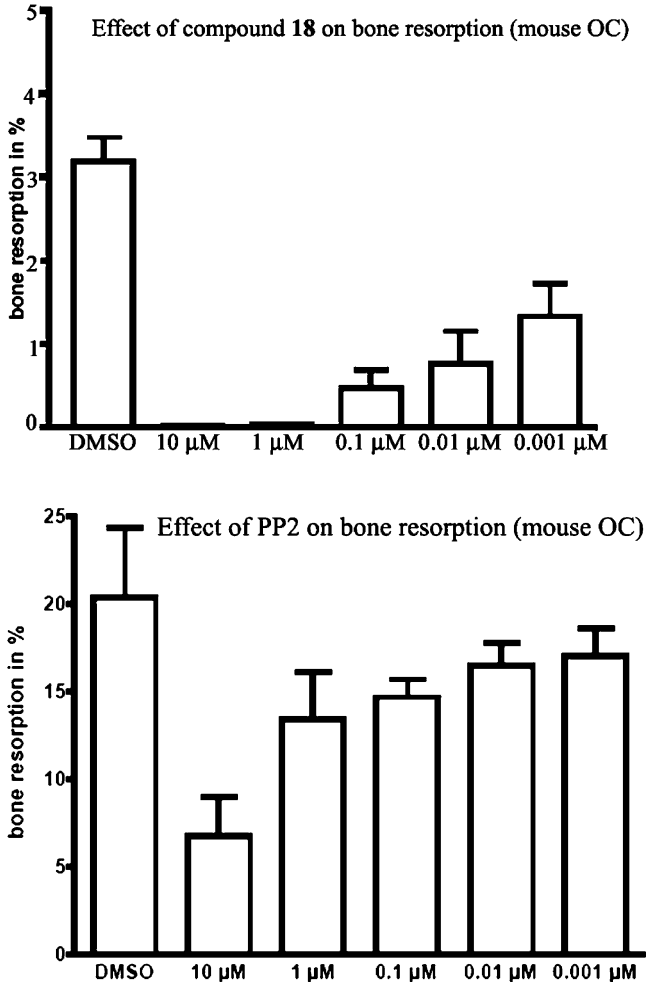

Figure 4. Effect of **18** and PP2 on bone resorption (mouse osteoclasts).

replicates. Despite such a limitation, this assay is widely recognized as the gold standard to assess the ability of compounds to inhibit bone resorption by osteoclasts.[27]

Experimental in Vivo Model. Experimental data collected for **18** are representative of a very interesting biological profile, in particular in terms of selectivity toward malignant cells and metabolic stability. Prompted by such results, we tested the activity of **18** on a human SaOS-2 xenograft tumor model in nude mice. In detail, SaOS-2 cells were injected sc in nude mice. The SaOS xenograft showed an appreciable growth starting from the fifth day after cell inoculation and doubled its volume in about 15 days. To evaluate the effect of **18** in such a preclinical experimental model of osteosarcoma, a treatment protocol was applied via the oral administration once daily of a suspension of the compound in cremphor vehicle. Interestingly, no appreciable sign of distress or loss of weight in mice was evidenced (data not shown). As a result, the administration of **18** (100 mg/kg) determined a significant reduction (about 37% with respect to control, at the endpoint) in xenograft growth, measured both as volume and as weight reduction (Figure 5). Also, the administration of a 50 mg/kg dose determined a smaller (about 15%) but significant reduction in tumor volume with respect to control (Figure 5).

To evaluate the inhibition of Src activation in vivo, xenograft tissues were processed for histologic evaluation of phospho-Src expression (Figure 6). Tumor cells both in the control group and in the treated group express c-Src (panels A and C), and its localization was prevalently detected in the cytoplasm of cells situated at the periphery of tumor mass. When the same

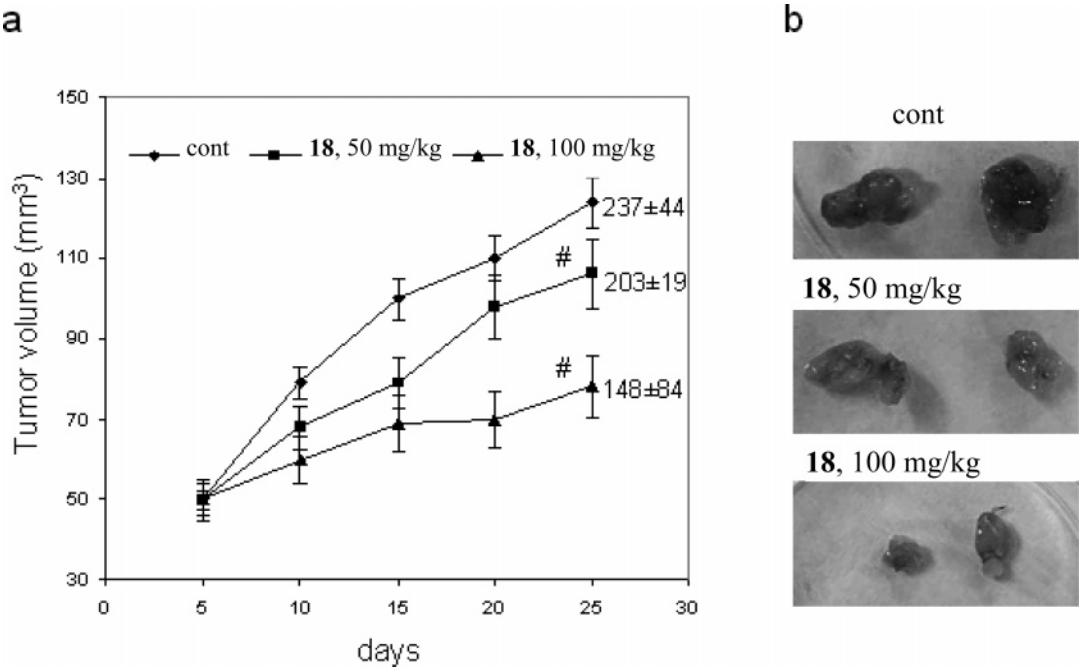

Figure 5. Inhibition of SaOS-2 xenograft growth. (a) Twelve mice were inoculated sc with tumor cells and were divided in three groups, each of four mice, receiving a daily oral administration of **18** (50 or 100 mg/kg) in cremphor vehicle. Tumor volumes were calculated every 5 days, and means ± SD were recorded. At the endpoint (26th day after cell injection), mice were sacrificed and tumors were measured and weighed. #, $P < 0.05$ according to Student's *t* test. (b) Example images of tumor excised from mice of each group at the endpoint.

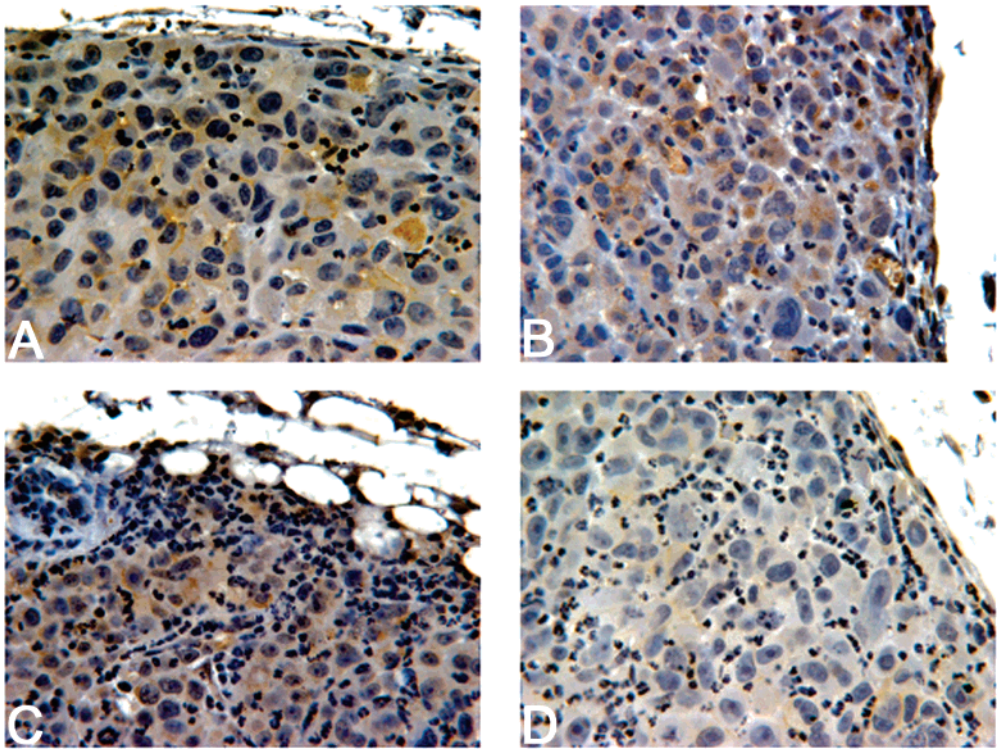

Figure 6. Immunohistologic analysis of xenografts. Tumor tissue sections were stained for the presence of total c-Src (A, C) and of phosphospecific-Src (pY418) (B, D). Representative images of tumor tissues from control xenografts and from 100 mg/kg **18**-treated group are shown in the left and right panels, respectively (magnification ×300). The brown staining indicates the presence of the antigen, and nuclei are stained with hematoxylin.

tissues were analyzed for the presence of activated phospho-Src, only a faint staining in the 100 mg/kg inhibitor-treated tumors was detected, with respect to the control tumor sections that, on the contrary, expressed high levels of the phospho-Src antigen (panels B and D).

Molecular Docking Calculations. Because **18** was found to inhibit Src phosphorylation through an ATP-competitive mechanism, it was docked into Src (entry 1y57 of the Protein Data Bank),[28] and the resulting complex was optimized by application of a computational protocol previously described.[17] Compound **18** (Figure 7) showed an orientation into the Src kinase domain similar to that found for congeneric compounds bearing an alkylthio substituent at C6.[17] In fact, previous simulations on pyrazolo-pyrimidine derivatives showed that the presence or the absence of an alkylthio substituent at position 6 of the molecular scaffold markedly influenced the binding mode of inhibitors

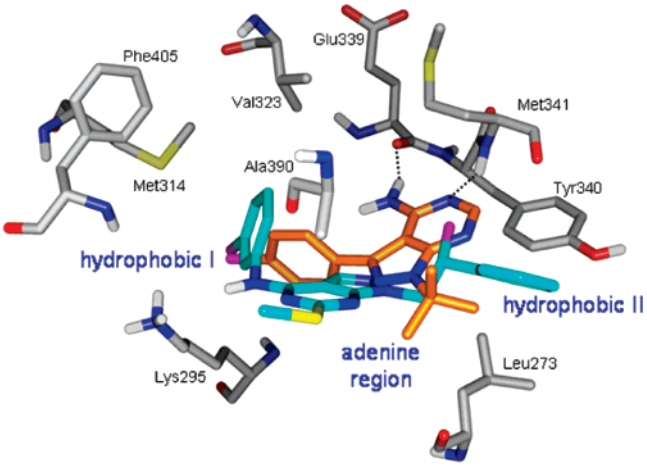

Figure 7. Graphical representation of the binding mode of **18** (cyan) into the ATP binding site of the active form of Src, in comparison to PP2 (orange). Only a few residues are displayed; nonpolar hydrogens are omitted, and hydrogen bonds are represented by black dotted lines.

within the ATP binding site. In detail, compounds unsubstituted at position 6 (such as **24**) showed an interaction pathway comparable to that of PP2, in terms of orientation, hydrogen bond pattern, and contacts with the hydrophobic regions I and II. On the other hand, the presence of an alkylthio substituent at position 6, as in **18**, induced a reorientation of the heterocyclic nucleus, leading to a different interaction pathway. In particular, the *m*-chlorophenylamino group was accommodated into the hydrophobic region I, whereas the N1 chain was partially inserted within the adenine region and directed toward the hydrophobic pocket II. The methylthio group was located into a hydrophobic region and was involved in favorable interactions with Ala390. As expected, in contrast to PP2, this compound was not engaged in any hydrogen bond. Interestingly, removal of the hydrogen bond network was not associated with loss of activity. In fact, despite the different orientation and the absence of hydrogen bonds, **18** showed an inhibitory activity toward Src comparable to that of PP2, suggesting that hydrogen bond contacts were not essential for activity and their stabilizing contribution could be replaced by additional hydrophobic interactions involving the alkylthio side chain. This result clearly suggested that lipophilic interactions resulting from full occupancy of hydrophobic regions I and II seemed to play a crucial role in the affinity of ligands toward Src.

Similarly to **18**, compounds **19**−**23** and **25**, bearing an anilino group at C4 in addition to the C6 alkylthio substituent, showed their C4 and N1 side chains within the hydrophobic regions I and II, respectively, resulting in a full and profitable occupancy of the two pockets. On the other hand, as previously described,[17] molecules bearing a larger substituent at C4 (benzylamino or phenylethylamino, such as **1**−**17**) assumed a different pose within the binding pocket, with C4 and N1 side chains in an opposite location with respect to **18** and other anilino analogues. As a general trend, this different accommodation was associated with less profitable interactions with amino acid residues and with a decreased affinity toward the target. In this context, compound **1** can be considered as an exception, showing one of the most interesting affinity values despite a binding mode common to less active compounds.

Conclusions

The new pyrazolo-pyrimidines reported here showed inhibitory properties toward Src phosphorylation, and one of them (**18**) proved to be an antiproliferative agent against malignant osteoblast SaOS-2 cells, with a very slight interference in the growth of normal osteoblasts. On the other hand, **18** markedly reduced bone resorption in mouse osteoclasts. Moreover, it was also able to inhibit the activity of Akt (known to be involved in a Src-dependent signaling pathway in osteosarcoma cells), but at the moment, we are still unable to totally exclude the involvement of other protein kinases in signaling pathways regulating osteoblasts and osteoclast cells. Finally, the metabolic stability of **18** prompted us to test it in vivo in mice; we found a significant decrease in xenograft growth measured as both volume and weight reduction, with respect to control. Additional experiments are ongoing for a further in vitro and in vivo characterization of **18** as a possible lead compound in the field of therapeutical tools for bone diseases.

Experimental Section

Chemistry. Starting materials were purchased from Aldrich-Italia (Milan, Italy). Melting points were determined with a Büchi 530 apparatus and are uncorrected. IR spectra were measured in KBr with a Perkin-Elmer 398 spectrophotometer. ^{1}H NMR spectra were recorded in a $(CD_3)_2SO$ solution on a Varian Gemini 200 (200 MHz) instrument. Chemical shifts are reported as δ (ppm) relative to TMS as internal standard, with J in hertz. ^{1}H patterns are described using the following abbreviations: s, singlet; d, doublet; t, triplet; q, quartet; sx, sextect; m, multiplet, br, broad.

All compounds were tested for purity by TLC (Merk, Silica gel 60 F_{254}, $CHCl_3$ as the eluant).

Analyses for C, H, N and S were within ±0.3% of the theoretical value.

Mass spectral (MS) data were obtained using an Agilent 1100 LC/MSD VL system (G1946C) with a 0.4 mL/min flow rate using a binary solvent system of 95:5 methyl alcohol/water. UV detection was monitored at 254 nm. Mass spectra were acquired in positive mode scanning over the mass range of 50−1500. The following ion source parameters were used: drying gas flow, 9 mL/min; nebulizer pressure, 40 psig; drying gas temperature, 350 °C.

Synthesis and experimental data of compounds **1**, **10**, **26a**, **27a**, **28a**, **29a**, **30a**, **30d**, **31a**, **31d**, and **32** were already reported by us.[17,19]

1-(4-Halophenyl)-2-hydrazinoethanols (26b,c). To hydrazine monohydrate (30 mL, 0.6 mol), heated at 100 °C was added the appropriate phenyloxirane (0.17 mmol). The solution was heated for 30 min at 100 °C, and the excess of hydrazine was removed under reduced pressure. The crude was purified by bulb to bulb distillation to obtain the pure products as pale yellow oils.

26b: yield, 85%; bp, 175−180 °C (0.6 mmHg); ^{1}H NMR, δ 2.62−2.87 (m, 2H, CH_2N), 3.55−3.87 (m, 4H, NH_2NH + OH, disappears with D_2O), 4.85−4.92 (m, 1H, CHO), 6.95−7.29 (m, 4H Ar); IR, 3323, 3280, 3250 (NH_2 + NH), 3400−3000 (OH) cm^{-1}. Anal. ($C_8H_{11}N_2FO$) C, H, N.

26c: yield, 80%; bp, 170−175 °C (0.6 mmHg); ^{1}H NMR, δ 2.65−2.88 (m, 2H, CH_2N), 3.56−3.90 (m, 4H, NH_2NH + OH, disappears with D_2O), 4.88−4.92 (m, 1H, CHO), 7.00−7.32 (m, 4H Ar); IR, 3320, 3290, 3250 (NH_2 + NH), 3350−2950 (OH) cm^{-1}. Anal. ($C_8H_{11}N_2ClO$) C, H, N.

Ethyl 5-Amino-1-[2-(4-halophenyl)-2-hydroxyethyl]-1*H*-pyrazole-4-carboxylates (27b,c). The starting hydrazine **26b** or **26c** (20 mmol) was added to a solution of ethyl(ethoxymethylene)cyanoacetate (3.38 g, 20 mmol) in anhydrous toluene (20 mL), and the mixture was heated at 80 °C for 8 h. The solution was then concentrated under reduced pressure to half of the volume and allowed to cool to room temperature. The pale yellow solids were filtered and recrystallized from toluene to afford **27b** and **27c** as white solids.

27b: yield, 70%; mp, 163−164 °C; ^{1}H NMR, δ 1.33 (t, J = 7.0, 3H, CH_3), 3.73 (br s, 1H, OH, disappears with D_2O), 3.90−4.15 (m, 2H, CH_2N), 4.29 (q, J = 7.0, 2H, CH_2O), 5.01−5.18 (m, 1H, CHO), 5.36 (br s, 2H, NH_2, disappears with D_2O), 7.03−7.40

(2 m, 4H Ar), 7.55 (s, 1H, H-3); IR, 3448, 3346 (NH_2), 3300−3000 (OH), 1685 (CO) cm^{-1}. Anal. ($C_{14}H_{16}N_3FO_3$) C, H, N.

27c: yield, 75%; mp, 168−169 °C; ^1H NMR, δ 1.38 (t, $J = 7.0$, 3H, CH_3), 3.56 (br s, 1H, OH, disappears with D_2O), 3.91−4.19 (m, 2H, CH_2N), 4.28 (q, $J = 7.0$, 2H, CH_2O), 5.05−5.18 (m, 1H, CHO), 5.33 (br s, 2H, NH_2, disappears with D_2O), 7.25−7.46 (m, 4H Ar), 7.59 (s, 1H, H-3); IR, 3412, 3291 (NH_2), 3219−3100 (OH), 1689 (CO) cm^{-1}. Anal. ($C_{14}H_{16}N_3ClO_3$) C, H, N.

Ethyl 5-{[(Benzoylamino)carbonothioyl]amino}-1-[2-(4-halophenyl)-2-hydroxyethyl]-1*H*-pyrazole-4-carboxylates (28b,c). A suspension of **27b** or **27c** (10 mmol) and benzoyl isothiocyanate (1.7 g, 11 mmol) in anhydrous THF (20 mL) was refluxed for 12 h. The solvent was evaporated under reduced pressure, and **28b** was crystallized by adding diethyl ether (30 mL) as a white solid, whereas **28c** was used as crude oil for the next reaction.

28b: yield, 85%; mp, 129−130 °C; ^1H NMR, δ 1.31 (t, $J = 7.0$, 3H, CH_3), 4.10−4.38 (m, 5H, $2CH_2$ + OH, 1H disappears with D_2O), 5.25−5.38 (m, 1H, CHO), 7.00−7.90 (m, 9H Ar), 8.05 (s, 1H, H-3), 9.36 (s, 1H, NH, disappears with D_2O), 12.16 (s, 1H, NH, disappears with D_2O); IR, 3444, 3261 (NH), 3190−2940 (OH), 1683 (CO) cm^{-1}. Anal. ($C_{22}H_{21}N_4FO_4S$) C, H, N, S.

1-[2-(4-Halophenyl)-2-hydroxyethyl]-6-thioxo-1,5,6,7-tetrahydro-4*H*-pyrazolo[3,4-*d*]pyrimidin-4-ones (29b,c). A solution of **28b** or **28c** (10 mmol) in 2 M NaOH (40 mL) was refluxed for 10 min and then diluted with H_2O (40 mL) and acidified with glacial acetic acid. After 12 h of standing in a refrigerator, a solid crystallized that was filtered and recrystallized from absolute ethanol to give **29b** and **29c** as white solids.

29b: yield, 75%; mp, 252−253 °C; ^1H NMR, δ 4.15−4.28 and 4.52−4.60 (2 m, 2H, CH_2N), 4.88−5.00 (m, 1H, CHO), 5.69 (s, 1H, OH, disappears with D_2O), 7.12−7.29 and 7.40−7.52 (2 m, 4H Ar), 7.98 (s, 1H, H-3), 12.20 (s, 1H, NH, disappears with D_2O), 13.36 (s, 1H, NH, disappears with D_2O); IR, 3315, 3200 (NH), 3320−2500 (OH), 1670 (CO) cm^{-1}. Anal. ($C_{13}H_{11}N_4FO_2S$) C, H, N, S.

29c: yield, 70%; mp, 249−250 °C; ^1H NMR, δ 4.13−4.65 (2 m, 2H, CH_2N), 4.84−5.00 (m, 1H, CHO), 5.71 (br s, 1H, OH, disappears with D_2O), 7.30−7.51 (m, 4H Ar), 7.97 (s, 1H, H-3), 12.19 (s, 1H, NH, disappears with D_2O), 13.38 (s, 1H, NH, disappears with D_2O); IR, 3390, 3220 (NH), 3100−2700 (OH), 1675 (CO) cm^{-1}. Anal. ($C_{13}H_{11}N_4ClO_2S$) C, H, N, S.

1-Substituted-6-(alkylthio)-1,5-dihydro-4*H*-pyrazolo[3,4-*d*]-pyrimidin-4-ones (30b,c,e). A solution of **29a**−**c** (10 mmol) and the appropriate alkyl iodide (50 mmol) in anhydrous THF (20 mL) was refluxed for 12 h. The solvent and the excess of alkyl iodide were removed by distillation under reduced pressure. The residue oil was crystallized by adding $CHCl_3$ (10 mL) and was purified by recrystallization with absolute ethanol to give **30b**,**c** as white solids. Compound **30e** was purified by column chromatography (silica gel), using a mixture of $CHCl_3/CH_3OH$ (8:2) as eluant.

30b: yield, 72%; mp, 217−218 °C; ^1H NMR, δ 2.51 (s, 3H, CH_3S), 4.24−4.50 (m, 2H, CH_2N), 4.55 (br s, 1H, OH, disappears with D_2O), 5.00−5.15 (m, 1H, CHO), 7.02−7.30 (m, 4H Ar), 7.96 (s, 1H, H-3), 12.33 (s, 1H, NH, disappears with D_2O); IR, 3418 (NH), 3120−2850 (OH), 1668 (CO) cm^{-1}. Anal. ($C_{14}H_{13}N_4FO_2S$) C, H, N, S.

30c: yield, 70%; mp, 210−211 °C; ^1H NMR, δ 2.84 (s, 3H, CH_3S), 4.22−4.48 (m, 2H, CH_2N), 4.94−5.16 (m, 1H, CHO), 5.76 (d, 1H, OH, disappears with D_2O), 7.07−7.22 (m, 4H Ar), 7.94 (s, 1H, H-3), 12.32 (s, 1H, NH, disappears with D_2O); IR, 3427 (NH), 3120−2850 (OH), 1667 (CO) cm^{-1}. Anal. ($C_{14}H_{13}N_4ClO_2S$) C, H, N, S.

30e: yield, 68%; mp, 165−166 °C; ^1H NMR, δ 0.91 (t, $J = 7.2$, 3H, CH_3), 1.61 (sext, $J = 7.2$, 2H, $CH_3\underline{CH_2}$), 3.01 (t, $J = 7.2$, 2H, CH_2S), 4.14−4.38 (m, 2H, CH_2N), 4.92−5.05 (m, 1H, CHO), 5.76 (d, 1H, OH, disappears with D_2O), 7.08−7.18 (m, 5H Ar), 7.87 (s, 1H, H-3), 12.20 (br s, 1H, NH, disappears with D_2O); IR, 3346 (NH), 3130−2900 (OH), 1692 (CO) cm^{-1}. Anal. ($C_{16}H_{18}N_4O_2S$) C, H, N, S.

1-Substituted-[4-chloro-6-(alkylthio)-1*H*-pyrazolo[3,4-*d*]pyrimidines (31b,c,e). The Vilsmeier complex, previously prepared from $POCl_3$ (6.13 g, 40 mmol) and anhydrous DMF (2.92 g, 40 mmol), was added to a suspension of **30b**,**c**,**e** (10 mmol) in $CHCl_3$ (20 mL), and the mixture was refluxed for 4 h. The solution was washed with H_2O (2 × 20 mL), dried ($MgSO_4$), filtered, and concentrated under reduced pressure. The crude oil was purified by column chromatography (Florisil 100−200 mesh), using diethyl ether as the eluant, to afford the pure product **31b**,**c**,**e** as white solids.

31b: yield, 70%; mp, 136−137 °C; ^1H NMR, δ 2.65 (s, 3H, CH_3S), 4.74−5.03 (m, 2H, CH_2N), 5.42−5.54 (m, 1H, CHCl), 6.96−7.08 and 7.29−7.44 (2 m, 4H Ar), 8.03 (s, 1H, H-3). Anal. ($C_{14}H_{11}N_4Cl_2F$ S) C, H, N, S.

31c: yield, 60%; mp, 142−143 °C; ^1H NMR, δ 2.65 (s, 3H, CH_3S), 4.74−5.03 (m, 2H, CH_2N), 5.42−5.53 (m, 1H, CHCl), 7.25−7.42 (m, 4H Ar), 8.03 (s, 1H, H-3). Anal. ($C_{14}H_{11}N_4Cl_3S$) C, H, N, S.

31e: yield, 65%; mp, 83−84 °C; ^1H NMR, δ 1.05 (t, $J = 7.2$, 3H, CH_3), 1.77 (sext, $J = 7.2$, 2H, $CH_3\underline{CH_2}$), 3.11 (t, $J = 7.2$, 2H, CH_2S), 4.64−4.95 (m, 2H, CH_2N), 5.32−5.46 (m, 1H, CHCl), 7.07−7.38 (m, 5H Ar), 7.95 (s, 1H, H-3). Anal. ($C_{16}H_{16}N_4Cl_2S$) C, H, N, S.

General Procedure for the 4-Amino-1*H*-pyrazolo[3,4-*d*]pyrimidines (2−9, 11−17). To a solution of **31a**, **31b**, **31c**, or **31d** (5 mmol) in anhydrous toluene (20 mL) was added the proper amine (20 mmol). The reaction mixture was stirred at room temperature for 36 h and then extracted with H_2O (2 × 20 mL). The organic phase was dried ($MgSO_4$), filtered, and concentrated under reduced pressure. The oil residue was crystallized by adding diethyl ether (10 mL) to give the final products as white solids.

2: yield, 73%; mp, 111−112 °C; ^1H NMR, δ 2.49 (s, 3H, CH_3S), 2.89 (t, $J = 7.0$, 2H, CH_2Ar), 3.75 (q, $J = 7.0$, 2H, $\underline{CH_2}NH$), 4.58−4.90 (m, 2H, CH_2N), 5.14 (br s, 1H, NH, disappears with D_2O), 5.34−5.51 (m, 1H, CHCl), 6.77−7.43 (m, 9H Ar), 7.64 (s, 1H, H-3); IR, 3248 (NH) cm^{-1}; MS (ESI), *m*/*z* 444.2 $[M + H]^+$, 464.2 $[M + Na]^+$. Anal. ($C_{22}H_{21}N_5ClFS$) C, H, N, S.

General Procedure for the 4-Anilino-1*H*-pyrazolo[3,4-*d*]-pyrimidines (18−25). To a solution of **31a**, **31b**, **31d**, and **31e** (5 mmol) in absolute ethanol (20 mL) was added the appropriate aniline (5 mmol), and the reaction mixture was stirred at reflux for 3 h. After cooling, a solid precipitated that was filtered, washed with H_2O, and recrystallized from absolute ethanol (10 mL) to give the final products as white solids. Compound **24** was prepared with the same procedure starting from **32**.

18: yield, 55%; mp, 102−103 °C; ^1H NMR, δ 2.52 (s, 3H, CH_3S), 4.58−4.90 (m, 2H, CH_2N), 5.34−5.44 (m, 1H, CHCl), 7.08−7.36 (m, 9H Ar), 7.57 (s, 1H, H-3); IR, 3277 (NH) cm^{-1}; MS (ESI), *m*/*z* 430.2 $[M + H]^+$, 452.2 $[M + Na]^+$. Anal. ($C_{20}H_{17}N_5Cl_2S$) C, H, N, S.

Biology. Human Osteosarcoma Cell Culture. The human osteosarcoma cell line SaOS-2 was obtained from ATCC (HTB-85) and cultured in Dulbecco's modified Eagle's medium (DMEM) (Sigma-Aldrich, St. Louis, MO) supplemented with 10% (v/v) fetal calf serum (FCS) (Sigma), at 37 °C, 2 mM L-glutamine (Sigma-Aldrich), penicillin (100 units/mL), and streptomycin (100 μg/mL), at 37 °C, in a humidified atmosphere of 7% CO_2/93% air.

Treatments. c-Src inhibitors were synthesized as described, dissolved in dimethyl sulfoxide (DMSO) (Sigma-Aldrich) at various concentrations, and diluted in cell culture medium prior to use. PP2 (Calbiochem, Darmstadt, Germany) was parallely used as a reference compound. Controls were carried out with DMSO concentrations corresponding to the higher doses of the test compounds. The final DMSO concentration did not exceed 0.2% (v/v) and did not affect the parameters analyzed. Cells were treated when at confluence.

Cell Viability. Cell proliferation was quantified by using the MTT ([3-(4,5-dimethylthiazol-2-yl)-2,5-diphenyltetrazolium bromide]) cell proliferation assay kit (Molecular Probe). Cells (about 50000, estimated with Thoma chamber) were seeded in a 96-multiwell plate with 10% (v/v) FCS, 2 mM L-glutamine, penicillin (100 units/mL), and streptomycin (100 μg/mL), grown for 48 h (confluence), and then exposed to test compounds (12.5 and 25 μM) for 24 or 48 h. The medium was then removed, and the cells

were incubated for 4 h with fresh medium in the presence of 1.2 mM MTT. Living cells reduce MTT to a strongly pigmented formazan crystals. After solubilization in DMSO, the absorbance of the formazan was measured with a microplate absorbance reader at 540 nm. The growth inhibitory activity of the compounds studied was compared with the activity of PP2, used at the same concentrations of compounds.

Cytotoxicity. The cytotoxic effect of compounds was evaluated by Trypan blue exclusion test. SaOS-2 cells plated in 24-well multiplates and grown in DMEM supplemented with 10% (v/v) FCS, 2 mM L-glutamine, penicillin (100 units/mL), and streptomycin (100 μg/mL). Cells were treated with PP2 and **18** at their respective IC_{50} concentrations (8 and 12.6 μM, respectively). IC_{50} values were determined on SaOS-2 cells after a 48 h of treatment at variable concentrations of the inhibitors (1, 3, 5, 12.5, 25, 50, and 100 μM). At the end of the treatment, cells were washed with PBS, detached by treatment with 0.05% (w/v) trypsin/0.02% (w/v) EDTA for 5 min at 37 °C and collected, stained with 0.05 mM Trypan blue solution in buffer saline (PBS), and observed by conventional light microscopy in a blind manner, using the Thoma chamber. The number of Trypan blue-positive cells was calculated and expressed as a percentage of the total number of cells of the negative control.

TUNEL Assay. The DNA strand breaks in the apoptotic cells were evaluated by the TUNEL in situ cell death detection kit according to the manufacturer's instruction (Roche Applied Science, Mannheim, Germany). Briefly, cells were fixed in 4% buffered paraformaldehyde (pH 7.4), washed (3 × 5 min) in PBS, blocked for 10 min with 3% H_2O_2 in methanol, subjected to permeabilization with 0.1% Triton X-100 in 0.1% (w/v) sodium citrate for 2 min, and incubated first for 10 min with an equilibration buffer and then with the reaction buffer containing the TdT enzyme for 60 min at 37 °C. Cells can be observed in a drop of PBS under a fluorescence microscope at this state, using an excitation wavelength in the range of 450−500 nm and detection in the range of 515−565 nm. Cells were treated with a solution of Convert-POD for 30 min in humidified atmosphere at 37 °C and washed three times with PBS. DAB substrate was added for 10 min and then, after three more washes with PBS, cells were mounted under a glass coverslip and analyzed under light microscope. For quantitative analysis, apoptotic and total cells were counted and their ratio was computed and represented in graph form.

Phosphorylation Assays. For phospho-SrcY416 detection, 10−20 μg of cell culture protein lysates, diluted in reducing buffer, were resolved by 12% SDS-PAGE and electrotransferred onto nitrocellulose for detection with specific antibodies. All antibodies employed were purchased from Cell Signaling Technology (Danvers, MA). Proteins were probed with primary antibodies overnight at 4 °C, followed by secondary antibodies for 1 h at rt. Detection was obtained by ImmunoStar HRP (Bio-Rad, Hercules, CA). Band areas were analyzed by scanning densitometry, using ImageScanner (Amersham Bioscience, Little Chalfont, U.K.) and Melanie II and PDQuest software (Bio-Rad). Band areas of phospho-SrcY416 were normalized toward those of total Src as an internal control.

Effects of Compounds on Bone Resorption (Mouse OC). Preparation of Bone. Preisolated bone from cattle was cut to slices with a thickness of 300−350 μm using a low-speed saw with a diamond blade. The slices were then cut to small equal squares (about 0.5 × 0.5 cm) with a scalpel. Cleaning of bone pieces was done by first washing three times with water and once with 70% ethanol in an ultrasound bath for 5 min. The pieces were then stored in 100% ethanol overnight. Sterilization was carried out using UV light in a laminar airflow workbench (LAF) for 15 min on each side. The sterilized bone pieces were finally fixed with sterile silicone grease to the wells of a 48-well culture plate (four pieces for each well) and preincubated in α-MEM + 10% heat-inactivated FCS for a minimum of 2 h.

Preparation of the Coculture. Osteoblasts and bone marrow cells from mice were cocultured to obtain osteoclasts from precursors by fusion and differentiation. Osteoblasts were quickly thawed at 37 °C in a water bath before the seeding of approximately 4 million cells to each culture plate. The culture plates were then incubated overnight, giving the osteoblasts time to attach to the bone surface.

Mice used for the isolation of bone of bone marrow cells were anesthetized with ether and killed by cervical dislocation (1 mouse for each 48-well plate). The femora were put in a Petri dish on ice containing sterile PBS, and the muscles were removed under sterile conditions. The ends of the bones were then cut off with a scalpel. The bone marrow was isolated from the contents of the bone with α-MEM + 10% FCS, using a sterile syringe and a small needle. The bone marrow and medium were then transferred to a 50 mL centrifuge tube and centrifuged for 5 min at 1500 rpm at 4 °C. The supernatant was removed and the pellet suspended in fresh medium, the amount of medium depending on the total number of wells.

The medium in the wells of the culture was removed, and 400 μL of bone marrow cell suspension was added to each well. In addition, 100 μL of medium with 1×10^{-5} M 1.25-$(OH)_2$-vitamin D_3 and 1×10^{-3} M PGE_2 was added to each well to reach an end concentration of 1×10^{-9} M 1.25-$(OH)_2$-vitamin-D_3 and 1×10^{-6} M PGE_2. The well plates were then incubated. After 48 h, the medium was changed and, after spending another 24 h in the incubator, the test substances (**18** and PP2) were added. The well plates were incubated for 48 h.

Staining of Bone Slices. Staining with toluidine blue makes it possible to see the resorption areas under a microscope.[29] To wash off the medium, residual silicone, and the layer of cells, the bone slices were placed in polypropylene tubes and cleaned with 70% isopropanol for 15 min in an ultrasound bath. The slices were stained with a 1% solution of toluidine blue for 4 min, before the superfluous dye was rinsed off with bidistilled water.

The stained slices of bone were examined under a light microscope, using a 10× magnifying objective lens. Digitalized images were acquired, and the areas of the resorption lacunae could be measured. The data were copied to Microsoft Excel, in which the final calculations were made according to the following: (1) total number of pits = sum of all pits in five photographs from each piece of bone; (2) total area = sum of the areas of all pits in the five photographs from each piece of bone; (3) average pit area = total area of pits/total number of pits; (4) % resorption = total area of pits × 100/6000000, where the value of 6 million was obtained by knowing that one field of vision equals 1.2 million μm^2 (because five fields of vision were photographed, the total number was 6 million); (5) % inibiton = [100 − (% resorption × 100)]/mean of % resorption of controls.

Metabolic Stability. Compound **18** was incubated at 1 μM with recombinant human cytochrome P450 3A4 with and without the cofactor NADPH for 1 h at 37 °C. Following precipitation of protein and filtration, percent remaining parent compound was detemined using UPLC-MS. Compounds with a percent remaining lower than 20% are classified as unstable, whereas compounds with percent remaining higher than 20% are classified as stable.

Animals and Experimental in Vivo Model. Male CD1 nude mice (Charles River, Milan, Italy) were maintained under the guidelines established by our Institution [University of L'Aquila, Medical School and Science and Technology School Board Regulations, complying with the Italian government regulation (n. 116, January 27, 1992) for the use of laboratory animals]. Before any invasive manipulation, mice were anesthetized with a mixture of ketamine (25 mg/mL)/xylazine (5 mg/mL). Xenografts were obtained by injecting sc 10^6 SAOS cells in 100 μL of 12 mg/mL Matrigel (Becton Dickinson, Franklin Lakes, NJ). Tumor growth was monitored daily by measuring the average tumor diameter. The volume of the tumor was expressed in cubic millimeters, according to the formula $4\pi r^3/3$.

Xenograft Histology. Subcutaneous tumors were fixed in 4% formaldehyde in 0.1 M phosphate buffer, pH 7.2, and embedded in paraffin. Slide-mounted tissue sections (4 μm thick) were deparaffinized in xylene and hydrated serially in 100, 95, and 80% ethanol. Endogenous peroxidases were quenched in 3% H_2O_2 in PBS for 1 h, and then slides were incubated with anti-human c-Src antibody or anti-human Src (pY418) phosphospecific antibody

(Biosource, Camarillo, CA) for 1 h at rt. Sections were washed three times in PBS, and antibody binding was revealed using the Sigma fast 3,3′-diaminobenzidine tablet set (Sigma, St. Louis, MO).

Acknowledgment. We gratefully acknowledge financial support provided by the Italian MIUR (PRIN 2004059221), the Fondazione Monte dei Paschi di Siena, and AIRC (cod. 1111). We are indebted to Dr. Doriano Fabbro (Novartis Institutes for Biomedical Research, Basel, Switzerland) for assays on the tyrosine kinase panel. We also acknowledge Prof. Gabriele Cruciani (University of Perugia, Italy) for kindly providing us with the program VolSurf. We thank Dr. Giovanni Gaviraghi (Sienabiotech, Siena, Italy) for helpful discussion and Antonella Nardi (University of Siena) for LC-MS analysis.

Supporting Information Available: Spectroscopic and elemental analysis data of some compounds. This material is available free of charge via the Internet at http://pubs.acs.org.

References

(1) Marzia, M.; Sims, N. A.; Voit, S.; Migliaccio, S.; Taranta, A.; Bernardini, S.; Faraggiana, T.; Yoneda, T.; Mundy, G. R.; Boyce, B. F.; Baron, R.; Teti, A. Decreased c-Src expression enhances osteoblast differentiation and bone formation. *J. Cell. Biol.* **2000**, *151*, 311−320.

(2) Almeida, M.; Han, L.; Bellido, T.; Manolagas, S. C.; Kousteni, S. Wnt proteins prevent apoptosis of both osteoblast progenitors and differentiated osteoblasts by β-catenin-dependent and -independent signaling cascades involving Src/Erk and phosphatidylinositol 3-kinase/Akt. *J. Biol. Chem.* **2005**, *280*, 41342−41351.

(3) Vertino, A. M.; Bula, C. M.; Chen, J. R.; Almeida, M.; Han, L.; Bellido, T.; Kousteni, S.; Norman, A. W.; Manolagas, S. C. Nongenotropic, anti-apoptotic signaling of $1\alpha,25(OH)_2$-vitamin D_3 and analogs through the ligand binding domain of the vitamin D receptor in osteoblasts and osteocytes. Mediation by Src, phophatidylinositol 3-, and JNK kinases. *J. Biol. Chem.* **2005**, *280*, 14130−14137.

(4) Soriano, P.; Montgomery, C.; Geske, R.; Bradley, A. Targeted disruption of the c-*src* proto-oncogene leads to osteopetrosis in mice. *Cell* **1991**, *64*, 693−702.

(5) Boyce, B. F.; Yoneda, T.; Lowe, C.; Soriano, P.; Mundy, G. R. Requirement of pp60c-*src* expression for osteoclasts to form ruffled borders and resorb bone in mice. *J. Clin. Invest.* **1992**, *90*, 1622−1627.

(6) Klein, B. Y.; Kerem, Z.; Rojansky, N. LDL induces SaOS2 osteoblasts death via Akt pathways responsive to a neutral sphingomyelinase inhibitor. *J. Cell. Biochem.* **2006**, *98*, 661−671.

(7) Azuma, K.; Tanaka, M.; Uekita, T.; Inoue, S.; Yokota, J.; Ouchi, Y.; Sakai, R. Tyrosine phosphorylation of paxillin affects the metastatic potential of human osteosarcoma. *Oncogene* **2005**, *24*, 4754−4764.

(8) Missbach, M.; Jeschke, M.; Feyen, J.; Muller, K.; Glatt, M.; Green, J.; Susa, M. A novel inhibitor of the tyrosine kinase Src suppresses phosphorylation of its major cellular substrates and reduces bone resorption in vitro and in rodent models in vivo. *Bone* **1999**, *24*, 437−449.

(9) Grey, A.; Reid, J. R. Emerging and potential therapies for osteoporosis. *Expert Opin. Invest. Drugs* **2005**, *14*, 265−278.

(10) Jin, U. H.; Kim, D. I.; Lee, T. K.; Lee, D. N.; Kim, J. K.; Lee, I. S.; Kim, C. H. Herbal formulation, Yukmi-jkhand-tang-Jahage, regulates bone resorption by inhibition of phosphorylation mediated by tirosine kinase Src and cyclooxygenase expression. *J. Ethnopharmacol.* **2006**, *106*, 333−343.

(11) Manara, M. C.; Bernard, G.; Lollini, P. L.; Nanni, P.; Zuntini, M.; Landuzzi, L.; Benini, S.; Lattanzi, G.; Sciandra, M.; Serra, M.; Colombo, M. P.; Bernard, A.; Picci, P.; Scotlandi, K. CD99 acts as an oncosuppressor in osteosarcoma. *Mol. Biol. Cell* **2006**, *17*, 1910−1921.

(12) Metcalf, C. A., III; van Schravendijk, M. R.; Dalgarno, D. C.; Sawyer, T. K. Targeting protein kinases for bone disease: discovery and development of Src inhibitors. *Curr. Pharm. Des.* **2002**, *8*, 2049−2075.

(13) Barrios Sosa, A. C.; Boschelli, D. H.; Wu, B.; Wang, Y.; Golas, J. M. Further studies on ethenyl and ethynyl-4-phenylamino-3-quinolinecarbonitriles: identification of subnanomolar Src kinase inhibitor. *Bioorg. Med. Chem. Lett.* **2005**, *15*, 1743−1747.

(14) Plé, P. A.; Green, T. P.; Hennequin, L. F.; Curwen, J.; Fennel, M.; Allen, J.; Lambert-van der Brempt, C.; Costello, G. Discovery of a new class of anilinoquinazoline inhibitors with high affinity and specificity for the tyrosine kinase domain of c-Src. *J. Med. Chem.* **2004**, *47*, 871−887.

(15) Altmann, E.; Widler, L.; Missbach, M. *N*(7)-substituted-5-aryl-pyrrolo[2,3-*d*]pyrimidines represent a versatile class of potent inhibitors of the tyrosine kinase c-Src. *Mini Rev. Med. Chem.* **2002**, *2*, 201−208.

(16) Hanke, J. H.; Gardner, J. P.; Dow, R. L.; Changelian, P. S.; Brissette, W. H.; Weringer, E. J.; Pollok, B. A.; Connelly, P. A. Discovery of a novel, potent, and Src family-selective tyrosine kinase inhibitor. Study of Lck- and FynT-dependent T cell activation. *J. Biol. Chem.* **1996**, *271*, 695−701.

(17) (a) Carraro, F.; Naldini, A.; Pucci, A.; Locatelli, G. A.; Maga, G.; Schenone, S.; Bruno, O.; Ranise, A.; Bondavalli, F.; Brullo, C.; Fossa, P.; Menozzi, G.; Mosti, L.; Modugno, M.; Tintori, C.; Manetti, F.; Botta, M. Pyrazolo[3,4-*d*]pyrimidines as potent antiproliferative and proapoptotic agents toward A431 and 8701-BC cells in culture via inhibition of c-Src phosphorylation. *J. Med. Chem.* **2006**, *49*, 1549−1561. (b) Angelucci, A.; Schenone, S.; Gravina, G. L.; Muzi, P.; Festuccia, C.; Vicentini, C.; Botta, M.; Bologna, M. Pyrazolo[3,4-*d*]pyrimidines c-Src inhibitors reduce epidermal growth factor-induced migration in prostate cancer cells. *Eur. J. Cancer* **2006**, *42*, 2838−2845.

(18) Bondavalli, F.; Botta, M.; Bruno, O.; Ciacci, A.; Corelli, F.; Fossa, P.; Lucacchini, A.; Manetti, F.; Martini, C.; Menozzi, G.; Mosti, L.; Schenone, S.; Tafi, A.; Trincavelli, M. L. Synthesis, molecular modeling studies, and pharmacological activity of selective A1 receptor antagonists. *J. Med. Chem.* **2002**, *45*, 4875−4887.

(19) Schenone, S.; Bruno, O.; Ranise, A.; Mosti, L.; Menozzi, G.; Fossa, P.; Donnini, S.; Santoro, A.; Ziche, M.; Manetti, F.; Botta, M. Antiproliferative activity of new 1-aryl-4-amino-1*H*-pyrazolo[3,4-*d*]-pyrimidine derivatives toward the human epidermoid carcinoma A431 cell line. *Eur. J. Med. Chem.* **2004**, *39*, 939−964.

(20) Although recent literature reports examples of compounds that could be used as comparators to validate enzymatic and cell models, PP2 was used as the reference compound for three main reasons: (i) because it was identified as a potent and selective inhibitor of Src tyrosine kinases (ref. 16), PP2 remains an appropriate reference compound when the activity toward Src is to be determined; (ii) a great number of literature reports have been published on PP2 during the past decade, giving us exhaustive information on its biological profile toward Src and other kinases; (iii) PP2 is a commercially and easily available compound.

(21) Maga, G. Manuscript in preparation.

(22) Further information is at the Volsurf website: http://www.moldiscovery.com/docs/volsurf.

(23) Synold, T. W.; Dussault, I.; Forman, B. M. The orphan nuclear receptor SXR coordinately regulates drug metabolism and efflux. *Nat. Med.* **2001**, *7*, 584−590.

(24) The activity of compounds **1**, **18**, **20**, and **22** was preliminarily assessed toward the following panel of kinases: HER-1, KDR, Flt-3, IGF-1R, Tek, c-Met, Ret, JAK-2, EphB4, FGFR-3-K650E, Axl, FAK, PKA, CDK2/A, Akt, PDK1, and B-Raf-V599E.

(25) Diaz-Montero, C. M.; Wygant, J. N.; McIntyre, B. W. PI3-K/Akt-mediated anoikis resistance of human osteosarcoma cells requires Src activation. *Eur. J. Cancer* **2006**, *42*, 1491−1500.

(26) Santucci, A. Manuscript in preparation.

(27) Takada, Y.; Kusuda, M.; Hiura, K.; Sato, T.; Mochizuki, H.; Nagao, Y.; Tomura, M.; Yahiro, M.; Hakeda, Y.; Kawashima, H. A simple method to assess osteoclast-mediated bone resorption using unfractionated bone cells. *Bone Miner.* **1992**, *17*, 347−359.

(28) Cowan-Jacob, S. W.; Fendrich, G.; Manley, P. W.; Jahnke, W.; Fabbro, D.; Liebetanz, J.; Meyer, T. The crystal structure of a c-Src complex in an active conformation suggests possible steps in c-Src activation. *Structure* **2005**, *13*, 861−871.

(29) Lakkakorpi, P.; Tuukkanen, J.; Hentunen, T.; Jarvelin, K.; Vaananen, K. Organization of osteoclast microfilaments during the attachment to bone surface in vitro. *J. Bone Miner. Res.* **1989**, *4*, 817−825.

(30) Ghose, A. K.; Viswanadhan, V. N.; Wendoloski, J. J. Prediction of hydrophobic (lipophilic) properties of small organic molecules using fragmental methods: analysis of ALOGP and CLOGP methods. *J. Phys. Chem.* **1998**, *102*, 3762−3772.

JM061449R